

Search for the decays $X(3872) \rightarrow K_S^0 K^\pm \pi^\mp$ and $K^*(892) \bar{K}$ at BESIII

M. Ablikim¹ , M. N. Achasov^{4,c} , P. Adlarson⁸¹ , X. C. Ai⁸⁶ , R. Aliberti³⁹ , A. Amoroso^{80A,80C} , Q. An^{77,64,\dagger},
Y. Bai⁶² , O. Bakina⁴⁰ , Y. Ban^{50,h} , H.-R. Bao⁷⁰ , X. L. Bao⁴⁹ , V. Batozskaya^{1,48} , K. Begzsuren³⁵,
N. Berger³⁹ , M. Berlowski⁴⁸ , M. B. Bertani^{30A} , D. Bettoni^{31A} , F. Bianchi^{80A,80C} , E. Bianco^{80A,80C},
A. Bortone^{80A,80C} , I. Boyko⁴⁰ , R. A. Briere⁵ , A. Brueggemann⁷⁴ , H. Cai⁸² , M. H. Cai^{42,k,l} , X. Cai^{1,64} ,
A. Calcaterra^{30A} , G. F. Cao^{1,70} , N. Cao^{1,70} , S. A. Cetin^{68A} , X. Y. Chai^{50,h} , J. F. Chang^{1,64} , T. T. Chang⁴⁷ ,
G. R. Che⁴⁷ , Y. Z. Che^{1,64,70} , C. H. Chen¹⁰ , Chao Chen⁶⁰ , G. Chen¹ , H. S. Chen^{1,70} , H. Y. Chen²¹ ,
M. L. Chen^{1,64,70} , S. J. Chen⁴⁶ , S. M. Chen⁶⁷ , T. Chen^{1,70} , W. Chen⁴⁹ , X. R. Chen^{34,70} , X. T. Chen^{1,70} ,
X. Y. Chen^{12,g} , Y. B. Chen^{1,64} , Y. Q. Chen¹⁶ , Z. K. Chen⁶⁵ , J. Cheng⁴⁹ , L. N. Cheng⁴⁷ , S. K. Choi¹¹ ,
X. Chu^{12,g} , G. Cibinetto^{31A} , F. Cossio^{80C} , J. Cotee-Meldrum⁶⁹ , H. L. Dai^{1,64} , J. P. Dai⁸⁴ ,
X. C. Dai⁶⁷ , A. Dbeyssi¹⁹ , R. E. de Boer³ , D. Dedovich⁴⁰ , C. Q. Deng⁷⁸ , Z. Y. Deng¹ , A. Denig³⁹ ,
I. Denisenko⁴⁰ , M. Destefanis^{80A,80C} , F. De Mori^{80A,80C} , X. X. Ding^{50,h} , Y. Ding⁴⁴ , Y. X. Ding³² ,
J. Dong^{1,64} , L. Y. Dong^{1,70} , M. Y. Dong^{1,64,70} , X. Dong⁸² , M. C. Du¹ , S. X. Du⁸⁶ , S. X. Du^{12,g} ,
X. L. Du⁸⁶ , Y. Y. Duan⁶⁰ , Z. H. Duan⁴⁶ , P. Egorov^{40,b} , G. F. Fan⁴⁶ , J. J. Fan²⁰ , Y. H. Fan⁴⁹ , J. Fang^{1,64} ,
J. Fang⁶⁵ , S. S. Fang^{1,70} , W. X. Fang¹ , Y. Q. Fang^{1,64,\dagger} , L. Fava^{80B,80C} , F. Feldbauer³ , G. Felici^{30A} ,
C. Q. Feng^{77,64} , J. H. Feng¹⁶ , L. Feng^{42,k,l} , Q. X. Feng^{42,k,l} , Y. T. Feng^{77,64} , M. Fritsch³ , C. D. Fu¹ ,
J. L. Fu⁷⁰ , Y. W. Fu^{1,70} , H. Gao⁷⁰ , Y. Gao^{77,64} , Y. N. Gao^{50,h} , Y. N. Gao²⁰ , Y. Y. Gao³² , Z. Gao⁴⁷ ,
S. Garbolino^{80C} , I. Garzia^{31A,31B} , L. Ge⁶² , P. T. Ge²⁰ , Z. W. Ge⁴⁶ , C. Geng⁶⁵ , E. M. Gersabeck⁷³ ,
A. Gilman⁷⁵ , K. Goetzen¹³ , J. D. Gong³⁸ , L. Gong⁴⁴ , W. X. Gong^{1,64} , W. Gradl³⁹ , S. Gramigna^{31A,31B} ,
M. Greco^{80A,80C} , M. D. Gu⁵⁵ , M. H. Gu^{1,64} , C. Y. Guan^{1,70} , A. Q. Guo³⁴ , J. N. Guo^{12,g} , L. B. Guo⁴⁵ ,
M. J. Guo⁵⁴ , R. P. Guo⁵³ , X. Guo⁵⁴ , Y. P. Guo^{12,g} , A. Guskov^{40,b} , J. Gutierrez²⁹ , T. T. Han¹ ,
F. Hanisch³ , K. D. Hao^{77,64} , X. Q. Hao²⁰ , F. A. Harris⁷¹ , C. Z. He^{50,h} , K. L. He^{1,70} , F. H. Heinsius³ ,
C. H. Heinz³⁹ , Y. K. Heng^{1,64,70} , C. Herold⁶⁶ , P. C. Hong³⁸ , G. Y. Hou^{1,70} , X. T. Hou^{1,70} , Y. R. Hou⁷⁰ ,
Z. L. Hou¹ , H. M. Hu^{1,70} , J. F. Hu^{61,j} , Q. P. Hu^{77,64} , S. L. Hu^{12,g} , T. Hu^{1,64,70} , Y. Hu¹ , Z. M. Hu⁶⁵ ,
G. S. Huang^{77,64} , K. X. Huang⁶⁵ , L. Q. Huang^{34,70} , P. Huang⁴⁶ , X. T. Huang⁵⁴ , Y. P. Huang¹ ,
Y. S. Huang⁶⁵ , T. Hussain⁷⁹ , N. Hüsken³⁹ , N. in der Wiesche⁷⁴ , J. Jackson²⁹ , Q. Ji¹ , Q. P. Ji²⁰ , W. Ji^{1,70} ,
X. B. Ji^{1,70} , X. L. Ji^{1,64} , X. Q. Jia⁵⁴ , Z. K. Jia^{77,64} , D. Jiang^{1,70} , H. B. Jiang⁸² , P. C. Jiang^{50,h} ,
S. J. Jiang¹⁰ , X. S. Jiang^{1,64,70} , J. B. Jiao⁵⁴ , J. K. Jiao³⁸ , Z. Jiao²⁵ , L. C. L. Jin¹ , S. Jin⁴⁶ , Y. Jin⁷² ,
M. Q. Jing^{1,70} , X. M. Jing⁷⁰ , T. Johansson⁸¹ , S. Kabana³⁶ , X. L. Kang¹⁰ , X. S. Kang⁴⁴ , B. C. Ke⁸⁶ ,
V. Khachatryan²⁹ , A. Khoukaz⁷⁴ , O. B. Kolcu^{68A} , B. Kopf³ , L. Kröger⁷⁴ , M. Kuessner³ , X. Kui^{1,70} ,
N. Kumar²⁸ , A. Kupsc^{48,81} , W. Kühn⁴¹ , Q. Lan⁷⁸ , W. N. Lan²⁰ , T. T. Lei^{77,64} , M. Lellmann³⁹ ,
T. Lenz³⁹ , C. Li⁵¹ , C. Li⁴⁷ , C. H. Li⁴⁵ , C. K. Li²¹ , D. M. Li⁸⁶ , F. Li^{1,64} , G. Li¹ , H. B. Li^{1,70} ,
H. J. Li²⁰ , H. L. Li⁸⁶ , H. N. Li^{61,j} , Hui Li⁴⁷ , J. R. Li⁶⁷ , J. S. Li⁶⁵ , J. W. Li⁵⁴ , K. Li¹ , K. L. Li^{42,k,l} ,
L. J. Li^{1,70} , Lei Li⁵² , M. H. Li⁴⁷ , M. R. Li^{1,70} , P. L. Li⁷⁰ , P. R. Li^{42,k,l} , Q. M. Li^{1,70} , Q. X. Li⁵⁴ ,
R. Li^{18,34} , S. X. Li¹² , Shanshan Li^{27,i} , T. Li⁵⁴ , T. Y. Li⁴⁷ , W. D. Li^{1,70} , W. G. Li^{1,\dagger} , X. Li^{1,70} ,
X. H. Li^{77,64} , X. K. Li^{50,h} , X. L. Li⁵⁴ , X. Y. Li^{1,9} , X. Z. Li⁶⁵ , Y. Li²⁰ , Y. G. Li⁷⁰ , Y. P. Li³⁸ ,
Z. H. Li⁴² , Z. J. Li⁶⁵ , Z. X. Li⁴⁷ , Z. Y. Li⁸⁴ , C. Liang⁴⁶ , H. Liang^{77,64} , Y. F. Liang⁵⁹ , Y. T. Liang^{34,70} ,
G. R. Liao¹⁴ , L. B. Liao⁶⁵ , M. H. Liao⁶⁵ , Y. P. Liao^{1,70} , J. Libby²⁸ , A. Limphirat⁶⁶ , D. X. Lin^{34,70} ,
L. Q. Lin⁴³ , T. Lin¹ , B. J. Liu¹ , B. X. Liu⁸² , C. X. Liu¹ , F. Liu¹ , F. H. Liu⁵⁸ , Feng Liu⁶ ,
G. M. Liu^{61,j} , H. Liu^{42,k,l} , H. B. Liu¹⁵ , H. M. Liu^{1,70} , Huihui Liu²² , J. B. Liu^{77,64} , J. J. Liu²¹ ,
K. Liu^{42,k,l} , K. Liu⁷⁸ , K. Y. Liu⁴⁴ , Ke Liu²³ , L. Liu⁴²

Y. Y. Peng^{42,k,l} , K. Peters^{13,e} , K. Petridis⁶⁹ , J. L. Ping⁴⁵ , R. G. Ping^{1,70} , S. Plura³⁹ , V. Prasad³⁸ ,
F. Z. Qi¹ , H. R. Qi⁶⁷ , M. Qi⁴⁶ , S. Qian^{1,64} , W. B. Qian⁷⁰ , C. F. Qiao⁷⁰ , J. H. Qiao²⁰ , J. J. Qin⁷⁸ ,
J. L. Qin⁶⁰ , L. Q. Qin¹⁴ , L. Y. Qin^{77,64} , P. B. Qin⁷⁸ , X. P. Qin⁴³ , X. S. Qin⁵⁴ , Z. H. Qin^{1,64} , J. F. Qiu¹ ,
Z. H. Qu⁷⁸ , J. Rademacker⁶⁹ , C. F. Redmer³⁹ , A. Rivetti^{80C} , M. Rolo^{80C} , G. Rong^{1,70} , S. S. Rong^{1,70} ,
F. Rosini^{30B,30C} , Ch. Rosner¹⁹ , M. Q. Ruan^{1,64} , N. Salone^{48,p} , A. Sarantsev^{40,d} , Y. Schelhaas³⁹ ,
K. Schoenning⁸¹ , M. Scodiggio^{31A} , W. Shan²⁶ , X. Y. Shan^{77,64} , Z. J. Shang^{42,k,l} , J. F. Shangguan¹⁷ ,
L. G. Shao^{1,70} , M. Shao^{77,64} , C. P. Shen^{12,g} , H. F. Shen^{1,9} , W. H. Shen⁷⁰ , X. Y. Shen^{1,70} , B. A. Shi⁷⁰ ,
H. Shi^{77,64} , J. L. Shi^{8,g} , J. Y. Shi¹ , S. Y. Shi⁷⁸ , X. Shi^{1,64} , H. L. Song^{77,64} , J. J. Song²⁰ , M. H. Song⁴² ,
T. Z. Song⁶⁵ , W. M. Song³⁸ , Y. X. Song^{50,h,m} , Zirong Song^{27,i} , S. Sosio^{80A,80C} , S. Spataro^{80A,80C} ,
S. Stansilau⁷⁵ , F. Stielcr³⁹ , S. S. Su⁴⁴ , G. B. Sun⁸² , G. X. Sun¹ , H. Sun⁷⁰ , H. K. Sun¹ , J. F. Sun²⁰ ,
K. Sun⁶⁷ , L. Sun⁸² , R. Sun⁷⁷ , S. S. Sun^{1,70} , T. Sun^{56,f} , W. Y. Sun⁵⁵ , Y. C. Sun⁸² , Y. H. Sun³² ,
Y. J. Sun^{77,64} , Y. Z. Sun¹ , Z. Q. Sun^{1,70} , Z. T. Sun⁵⁴ , C. J. Tang⁵⁹ , G. Y. Tang¹ , J. Tang⁶⁵ , J. J. Tang^{77,64} ,
L. F. Tang⁴³ , Y. A. Tang⁸² , L. Y. Tao⁷⁸ , M. Tat⁷⁵ , J. X. Teng^{77,64} , J. Y. Tian^{77,64} , W. H. Tian⁶⁵ ,
Y. Tian³⁴ , Z. F. Tian⁸² , I. Uman^{68B} , B. Wang¹ , B. Wang⁶⁵ , Bo Wang^{77,64} , C. Wang^{42,k,l} , C. Wang²⁰ ,
Cong Wang²³ , D. Y. Wang^{50,h} , H. J. Wang^{42,k,l} , H. R. Wang⁸³ , J. Wang¹⁰ , J. J. Wang⁸² , J. P. Wang³⁷ ,
K. Wang^{1,64} , L. L. Wang¹ , L. W. Wang³⁸ , M. Wang⁵⁴ , M. Wang^{77,64} , N. Y. Wang⁷⁰ , S. Wang^{42,k,l} ,
Shun Wang⁶³ , T. Wang^{12,g} , T. J. Wang⁴⁷ , W. Wang⁶⁵ , W. P. Wang³⁹ , X. Wang^{50,h} , X. F. Wang^{42,k,l} ,
X. L. Wang^{12,g} , X. N. Wang^{1,70} , Xin Wang^{27,i} , Y. Wang¹ , Y. D. Wang⁴⁹ , Y. F. Wang^{1,9,70} ,
Y. H. Wang^{42,k,l} , Y. J. Wang^{77,64} , Y. L. Wang²⁰ , Y. N. Wang⁴⁹ , Y. N. Wang⁸² , Yaqian Wang¹⁸ , Yi Wang⁶⁷ ,
Yuan Wang^{18,34} , Z. Wang^{1,64} , Z. Wang⁴⁷ , Z. L. Wang² , Z. Q. Wang^{12,g} , Z. Y. Wang^{1,70} , Ziyi Wang⁷⁰ ,
D. Wei⁴⁷ , D. H. Wei¹⁴ , H. R. Wei⁴⁷ , F. Weidner⁷⁴ , S. P. Wen¹ , U. Wiedner³ , G. Wilkinson⁷⁵ , M. Wolke⁸¹ ,
J. F. Wu^{1,9} , L. H. Wu¹ , L. J. Wu²⁰ , Lianjie Wu²⁰ , S. G. Wu^{1,70} , S. M. Wu⁷⁰ , X. W. Wu⁷⁸ , Y. J. Wu³⁴ ,
Z. Wu^{1,64} , L. Xia^{77,64} , B. H. Xiang^{1,70} , D. Xiao^{42,k,l} , G. Y. Xiao⁴⁶ , H. Xiao⁷⁸ , Y. L. Xiao^{12,g} ,
Z. J. Xiao⁴⁵ , C. Xie⁴⁶ , K. J. Xie^{1,70} , Y. Xie⁵⁴ , Y. G. Xie^{1,64} , Y. H. Xie⁶ , Z. P. Xie^{77,64} , T. Y. Xing^{1,70} ,
C. J. Xu⁶⁵ , G. F. Xu¹ , H. Y. Xu² , M. Xu^{77,64} , Q. J. Xu¹⁷ , Q. N. Xu³² , T. D. Xu⁷⁸ , X. P. Xu⁶⁰ ,
Y. Xu^{12,g} , Y. C. Xu⁸³ , Z. S. Xu⁷⁰ , F. Yan²⁴ , L. Yan^{12,g} , W. B. Yan^{77,64} , W. C. Yan⁸⁶ , W. H. Yan⁶ ,
W. P. Yan²⁰ , X. Q. Yan^{12,g} , X. Q. Yan^{12,g} , Y. Y. Yan⁶⁶ , H. J. Yang^{56,f} , H. L. Yang³⁸ , H. X. Yang¹ ,
J. H. Yang⁴⁶ , R. J. Yang²⁰ , Y. Yang^{12,g} , Y. H. Yang⁴⁶ , Y. Q. Yang¹⁰ , Y. Z. Yang²⁰ , Z. P. Yao⁵⁴ ,
M. Ye^{1,64} , M. H. Ye^{9,i} , Z. J. Ye^{61,j} , Junhao Yin⁴⁷ , Z. Y. You⁶⁵ , B. X. Yu^{1,64,70} , C. X. Yu⁴⁷ , G. Yu¹³ ,
J. S. Yu^{27,i} , L. W. Yu^{12,g} , T. Yu⁷⁸ , X. D. Yu^{50,h} , Y. C. Yu⁸⁶ , Y. C. Yu⁴² , C. Z. Yuan^{1,70} , H. Yuan^{1,70} ,
J. Yuan³⁸ , J. Yuan⁴⁹ , L. Yuan² , M. K. Yuan^{12,g} , S. H. Yuan⁷⁸ , Y. Yuan^{1,70} , C. X. Yue⁴³ , Ying Yue²⁰ ,
A. A. Zafar⁷⁹ , F. R. Zeng⁵⁴ , S. H. Zeng⁶⁹ , X. Zeng^{12,g} , Yujie Zeng⁶⁵ , Y. J. Zeng^{1,70} , Y. C. Zhai⁵⁴ ,
Y. H. Zhan⁶⁵ , Shunan Zhang⁷⁵ , B. L. Zhang^{1,70} , B. X. Zhang^{1,†} , D. H. Zhang⁴⁷ , G. Y. Zhang²⁰ ,
G. Y. Zhang^{1,70} , H. Zhang^{77,64} , H. Zhang⁸⁶ , H. C. Zhang^{1,64,70} , H. H. Zhang⁶⁵ , H. Q. Zhang^{1,64,70} ,
H. R. Zhang^{77,64} , H. Y. Zhang^{1,64} , J. Zhang⁶⁵ , J. J. Zhang⁵⁷ , J. L. Zhang²¹ , J. Q. Zhang⁴⁵ , J. S. Zhang^{12,g} ,
J. W. Zhang^{1,64,70} , J. X. Zhang^{42,k,l} , J. Y. Zhang¹ , J. Z. Zhang^{1,70} , Jianyu Zhang⁷⁰ , L. M. Zhang⁶⁷ ,
Lei Zhang⁴⁶ , N. Zhang³⁸ , P. Zhang^{1,9} , Q. Zhang²⁰ , Q. Y. Zhang³⁸ , R. Y. Zhang^{42,k,l} , S. H. Zhang^{1,70} ,
Shulei Zhang^{27,i} , X. M. Zhang¹ , X. Y. Zhang⁵⁴ , Y. Zhang¹ , Y. Zhang⁷⁸ , Y. T. Zhang⁸⁶ , Y. H. Zhang^{1,64} ,
Y. P. Zhang^{77,64} , Z. D. Zhang¹ , Z. H. Zhang¹ , Z. L. Zhang³⁸ , Z. L. Zhang⁶⁰ , Z. X. Zhang²⁰ , Z. Y. Zhang⁸² ,
Z. Y. Zhang⁴⁷ , Z. Y. Zhang⁴⁹ , Zh. Zh. Zhang²⁰ , G. Zhao¹ , J. Y. Zhao^{1,70} , J. Z. Zhao^{1,64} , L. Zhao¹ ,
L. Zhao^{77,64} , M. G. Zhao⁴⁷

- ⁷ *Central South University, Changsha 410083, People's Republic of China*
- ⁸ *Chengdu University of Technology, Chengdu 610059, People's Republic of China*
- ⁹ *China Center of Advanced Science and Technology, Beijing 100190, People's Republic of China*
- ¹⁰ *China University of Geosciences, Wuhan 430074, People's Republic of China*
- ¹¹ *Chung-Ang University, Seoul, 06974, Republic of Korea*
- ¹² *Fudan University, Shanghai 200433, People's Republic of China*
- ¹³ *GSI Helmholtzcentre for Heavy Ion Research GmbH, D-64291 Darmstadt, Germany*
- ¹⁴ *Guangxi Normal University, Guilin 541004, People's Republic of China*
- ¹⁵ *Guangxi University, Nanning 530004, People's Republic of China*
- ¹⁶ *Guangxi University of Science and Technology, Liuzhou 545006, People's Republic of China*
- ¹⁷ *Hangzhou Normal University, Hangzhou 310036, People's Republic of China*
- ¹⁸ *Hebei University, Baoding 071002, People's Republic of China*
- ¹⁹ *Helmholtz Institute Mainz, Staudinger Weg 18, D-55099 Mainz, Germany*
- ²⁰ *Henan Normal University, Xinxiang 453007, People's Republic of China*
- ²¹ *Henan University, Kaifeng 475004, People's Republic of China*
- ²² *Henan University of Science and Technology, Luoyang 471003, People's Republic of China*
- ²³ *Henan University of Technology, Zhengzhou 450001, People's Republic of China*
- ²⁴ *Hengyang Normal University, Hengyang 421001, People's Republic of China*
- ²⁵ *Huangshan College, Huangshan 245000, People's Republic of China*
- ²⁶ *Hunan Normal University, Changsha 410081, People's Republic of China*
- ²⁷ *Hunan University, Changsha 410082, People's Republic of China*
- ²⁸ *Indian Institute of Technology Madras, Chennai 600036, India*
- ²⁹ *Indiana University, Bloomington, Indiana 47405, USA*
- ³⁰ *INFN Laboratori Nazionali di Frascati, (A)INFN Laboratori Nazionali di Frascati, I-00044, Frascati, Italy; (B)INFN Sezione di Perugia, I-06100, Perugia, Italy; (C)University of Perugia, I-06100, Perugia, Italy*
- ³¹ *INFN Sezione di Ferrara, (A)INFN Sezione di Ferrara, I-44122, Ferrara, Italy; (B)University of Ferrara, I-44122, Ferrara, Italy*
- ³² *Inner Mongolia University, Hohhot 010021, People's Republic of China*
- ³³ *Institute of Business Administration, Karachi,*
- ³⁴ *Institute of Modern Physics, Lanzhou 730000, People's Republic of China*
- ³⁵ *Institute of Physics and Technology, Mongolian Academy of Sciences, Peace Avenue 54B, Ulaanbaatar 13330, Mongolia*
- ³⁶ *Instituto de Alta Investigación, Universidad de Tarapacá, Casilla 7D, Arica 1000000, Chile*
- ³⁷ *Jiangsu Ocean University, Lianyungang 222000, People's Republic of China*
- ³⁸ *Jilin University, Changchun 130012, People's Republic of China*
- ³⁹ *Johannes Gutenberg University of Mainz, Johann-Joachim-Becher-Weg 45, D-55099 Mainz, Germany*
- ⁴⁰ *Joint Institute for Nuclear Research, 141980 Dubna, Moscow region, Russia*
- ⁴¹ *Justus-Liebig-Universitaet Giessen, II. Physikalisches Institut, Heinrich-Buff-Ring 16, D-35392 Giessen, Germany*
- ⁴² *Lanzhou University, Lanzhou 730000, People's Republic of China*
- ⁴³ *Liaoning Normal University, Dalian 116029, People's Republic of China*
- ⁴⁴ *Liaoning University, Shenyang 110036, People's Republic of China*
- ⁴⁵ *Nanjing Normal University, Nanjing 210023, People's Republic of China*
- ⁴⁶ *Nanjing University, Nanjing 210093, People's Republic of China*
- ⁴⁷ *Nankai University, Tianjin 300071, People's Republic of China*
- ⁴⁸ *National Centre for Nuclear Research, Warsaw 02-093, Poland*
- ⁴⁹ *North China Electric Power University, Beijing 102206, People's Republic of China*
- ⁵⁰ *Peking University, Beijing 100871, People's Republic of China*
- ⁵¹ *Qufu Normal University, Qufu 273165, People's Republic of China*
- ⁵² *Renmin University of China, Beijing 100872, People's Republic of China*
- ⁵³ *Shandong Normal University, Jinan 250014, People's Republic of China*
- ⁵⁴ *Shandong University, Jinan 250100, People's Republic of China*
- ⁵⁵ *Shandong University of Technology, Zibo 255000, People's Republic of China*
- ⁵⁶ *Shanghai Jiao Tong University, Shanghai 200240, People's Republic of China*
- ⁵⁷ *Shanxi Normal University, Linfen 041004, People's Republic of China*

- ⁵⁸ Shanxi University, Taiyuan 030006, People's Republic of China
- ⁵⁹ Sichuan University, Chengdu 610064, People's Republic of China
- ⁶⁰ Soochow University, Suzhou 215006, People's Republic of China
- ⁶¹ South China Normal University, Guangzhou 510006, People's Republic of China
- ⁶² Southeast University, Nanjing 211100, People's Republic of China
- ⁶³ Southwest University of Science and Technology, Mianyang 621010, People's Republic of China
- ⁶⁴ State Key Laboratory of Particle Detection and Electronics, Beijing 100049, Hefei 230026, People's Republic of China
- ⁶⁵ Sun Yat-Sen University, Guangzhou 510275, People's Republic of China
- ⁶⁶ Suranaree University of Technology, University Avenue 111, Nakhon Ratchasima 30000, Thailand
- ⁶⁷ Tsinghua University, Beijing 100084, People's Republic of China
- ⁶⁸ Turkish Accelerator Center Particle Factory Group, (A)Istinye University, 34010, Istanbul, Turkey; (B)Near East University, Nicosia, North Cyprus, 99138, Mersin 10, Turkey
- ⁶⁹ University of Bristol, H H Wills Physics Laboratory, Tyndall Avenue, Bristol, BS8 1TL, UK
- ⁷⁰ University of Chinese Academy of Sciences, Beijing 100049, People's Republic of China
- ⁷¹ University of Hawaii, Honolulu, Hawaii 96822, USA
- ⁷² University of Jinan, Jinan 250022, People's Republic of China
- ⁷³ University of Manchester, Oxford Road, Manchester, M13 9PL, United Kingdom
- ⁷⁴ University of Muenster, Wilhelm-Klemm-Strasse 9, 48149 Muenster, Germany
- ⁷⁵ University of Oxford, Keble Road, Oxford OX13RH, United Kingdom
- ⁷⁶ University of Science and Technology Liaoning, Anshan 114051, People's Republic of China
- ⁷⁷ University of Science and Technology of China, Hefei 230026, People's Republic of China
- ⁷⁸ University of South China, Hengyang 421001, People's Republic of China
- ⁷⁹ University of the Punjab, Lahore-54590, Pakistan
- ⁸⁰ University of Turin and INFN, (A)University of Turin, I-10125, Turin, Italy; (B)University of Eastern Piedmont, I-15121, Alessandria, Italy; (C)INFN, I-10125, Turin, Italy
- ⁸¹ Uppsala University, Box 516, SE-75120 Uppsala, Sweden
- ⁸² Wuhan University, Wuhan 430072, People's Republic of China
- ⁸³ Yantai University, Yantai 264005, People's Republic of China
- ⁸⁴ Yunnan University, Kunming 650500, People's Republic of China
- ⁸⁵ Zhejiang University, Hangzhou 310027, People's Republic of China
- ⁸⁶ Zhengzhou University, Zhengzhou 450001, People's Republic of China
- † Deceased
- ^a Also at Bogazici University, 34342 Istanbul, Turkey
- ^b Also at the Moscow Institute of Physics and Technology, Moscow 141700, Russia
- ^c Also at the Novosibirsk State University, Novosibirsk, 630090, Russia
- ^d Also at the NRC "Kurchatov Institute", PNPI, 188300, Gatchina, Russia
- ^e Also at Goethe University Frankfurt, 60323 Frankfurt am Main, Germany
- ^f Also at Key Laboratory for Particle Physics, Astrophysics and Cosmology, Ministry of Education; Shanghai Key Laboratory for Particle Physics and Cosmology; Institute of Nuclear and Particle Physics, Shanghai 200240, People's Republic of China
- ^g Also at Key Laboratory of Nuclear Physics and Ion-beam Application (MOE) and Institute of Modern Physics, Fudan University, Shanghai 200443, People's Republic of China
- ^h Also at State Key Laboratory of Nuclear Physics and Technology, Peking University, Beijing 100871, People's Republic of China
- ⁱ Also at School of Physics and Electronics, Hunan University, Changsha 410082, China
- ^j Also at Guangdong Provincial Key Laboratory of Nuclear Science, Institute of Quantum Matter, South China Normal University, Guangzhou 510006, China
- ^k Also at MOE Frontiers Science Center for Rare Isotopes, Lanzhou University, Lanzhou 730000, People's Republic of China
- ^l Also at Lanzhou Center for Theoretical Physics, Lanzhou University, Lanzhou 730000, People's Republic of China
- ^m Also at Ecole Polytechnique Federale de Lausanne (EPFL), CH-1015 Lausanne, Switzerland
- ⁿ Also at Helmholtz Institute Mainz, Staudinger Weg 18, D-55099 Mainz, Germany
- ^o Also at Hangzhou Institute for Advanced Study, University of Chinese Academy of Sciences, Hangzhou 310024, China
- ^p Currently at Silesian University in Katowice, Chorzow, 41-500, Poland
- ^q Also at Applied Nuclear Technology in Geosciences Key Laboratory of Sichuan Province,

Using a 10.9 fb^{-1} data sample collected by the BESIII detector at center-of-mass energies from 4.16 to 4.34 GeV, we search for the charmless decays $X(3872) \rightarrow K_S^0 K^\pm \pi^\mp$ and $K^*(892)\bar{K}$, where the $X(3872)$ is produced via the radiative process $e^+e^- \rightarrow \gamma X(3872)$. No significant signal is observed. We set upper limits on the relative branching fractions $\mathcal{B}[X(3872) \rightarrow K_S^0 K^\pm \pi^\mp]/\mathcal{B}[X(3872) \rightarrow \pi^+\pi^- J/\psi] < 0.07$ and $\mathcal{B}[X(3872) \rightarrow K^*(892)\bar{K}]/\mathcal{B}[X(3872) \rightarrow \pi^+\pi^- J/\psi] < 0.10$ at the 90% confidence level. Additionally, upper limits on the product of the cross section $\sigma[e^+e^- \rightarrow \gamma X(3872)]$ and the branching fractions $\mathcal{B}[X(3872) \rightarrow K_S^0 K^\pm \pi^\mp]$ and $\mathcal{B}[X(3872) \rightarrow K^*(892)\bar{K}]$ are reported at each energy point. In all cases, $K^*(892)\bar{K}$ refers to the sum of the modes $K^*(892)^+ K^- + \text{c.c.}$ and $K^*(892)^0 \bar{K}^0 + \text{c.c.}$, where c.c. denotes the corresponding charge-conjugate modes.

I. INTRODUCTION

The $X(3872)$, which is a strong candidate for an exotic hadron, was first observed by the Belle Collaboration in 2003 in the decay $B^\pm \rightarrow K^\pm X(3872)$ with $X(3872) \rightarrow \pi^+\pi^- J/\psi$ [1], and was subsequently confirmed by CDF [2], D0 [3], BaBar [4], LHCb [5] and BESIII [6]. After more than 20 years of study, it is established as a narrow resonance with a Breit-Wigner width of $1.19 \pm 0.21 \text{ MeV}/c^2$ [7], a mass of $3871.64 \pm 0.06 \text{ MeV}$ (which is very close to the $D^0 \bar{D}^{*0}$ threshold), and quantum numbers $J^{PC} = 1^{++}$ [8]. Several decay channels have been well measured, including $\gamma J/\psi$, $\pi^+\pi^- J/\psi$, and $\omega J/\psi$, and it has also been found to strongly couple to $D^0 \bar{D}^{*0}$ [9–12]. All of these observed decay modes of the $X(3872)$ contain a charm quark and an anti-charm quark in the final state, suggesting it has a minimal quark content of $c\bar{c}$. Given its measured quantum numbers and mass, the closest match in the potential model is the $\chi_{c1}(2P)$ state. However, the mass of the $X(3872)$ is lower than theoretical predictions for the $\chi_{c1}(2P)$, and significant isospin violation is observed in its decays, with the ratio $\mathcal{B}[X(3872) \rightarrow \pi^+\pi^-\pi^0 J/\psi]/\mathcal{B}[X(3872) \rightarrow \pi^+\pi^- J/\psi] = 1.6_{-0.3}^{+0.4} \pm 0.2$ [13]. These features are unexpected for a pure $c\bar{c}$ state, indicating that the $X(3872)$ may possess a more complex substructure, making it a candidate for an exotic hadron. Currently, various theoretical explanations exist for its nature, including interpretations as a charmonium state [14–16], a hadronic molecule [17–19], a tetraquark [20, 21], or a mixture of these components [22–24].

Investigating the decay patterns of the $X(3872)$, such as the possible role of charmless decays, is helpful for understanding its underlying structure. The decay with a final state of $K_S^0 K^\pm \pi^\mp$ is a charmless light hadron decay and has been extensively studied in various charmonium decays [25–29], so an experimental measurement of $X(3872) \rightarrow K_S^0 K^\pm \pi^\mp$ is valuable. Additionally, the decays $X(3872) \rightarrow K^*(892)\bar{K}$ are charmless VP decays, where V and P denote vector and pseudoscalar mesons, respectively. Assuming the $X(3872)$ is a $\bar{D}D^* + \text{c.c.}$ molecular bound state, which includes both neutral components ($\bar{D}^0 D^{*0} + \text{c.c.}$) and charged components ($D^- D^{*+} + \text{c.c.}$), a theoretical prediction [30] based on intermediate $\bar{D}D^* + \text{c.c.}$ meson loops estimates the branching fractions for $X(3872) \rightarrow VP$ decay modes. The numerical results are highly sensitive to the model parameter α that governs the intermediate charmed-meson loops. The value of α

is typically constrained by comparing the theoretical predictions with the corresponding experimental measurements. In particular, the $X(3872) \rightarrow K^*(892)\bar{K}$ branching fraction is calculated to be in a range of $(0.08\text{--}3.99) \times 10^{-2}$ (with pure neutral components), $(0.17\text{--}8.65) \times 10^{-2}$ (with the neutral components dominant) or $(0.24\text{--}13.29) \times 10^{-2}$ (with equal neutral and charged components) [30].

This analysis searches for the processes $e^+e^- \rightarrow \gamma X(3872) \rightarrow \gamma(K_S^0 K^\pm \pi^\mp)$ and $e^+e^- \rightarrow \gamma X(3872) \rightarrow \gamma(K^*(892)\bar{K})$, where $K^*(892)\bar{K}$ refers to the combinations $K^*(892)^+ K^- + \text{c.c.}$ and $K^*(892)^0 \bar{K}^0 + \text{c.c.}$. We analyze a data sample collected by the BESIII detector at center-of-mass (c.m.) energies ranging from 4.16 to 4.34 GeV with a total integrated luminosity of 10.9 fb^{-1} . The neutral state $K^*(892)^0(\bar{K}^*(892)^0)$ is reconstructed through its decay to $K^+\pi^-(K^-\pi^+)$, while the charged state $K^*(892)^+(K^*(892)^-)$ is reconstructed via $K^0\pi^+(\bar{K}^0\pi^-)$. Both decay channels, namely $X(3872) \rightarrow K_S^0 K^\pm \pi^\mp$ and $X(3872) \rightarrow K^*(892)\bar{K}$, yield the same final state $K_S^0 K^\pm \pi^\mp$. The K_S^0 is reconstructed via its decay to $\pi^+\pi^-$.

II. BESIII DETECTOR AND MONTE CARLO SIMULATION

The BESIII detector [31] records symmetric e^+e^- collisions provided by the BEPCII storage ring [32] in the c.m. energy range from 1.84 to 4.95 GeV, with a peak luminosity of $1.1 \times 10^{33} \text{ cm}^{-2}\text{s}^{-1}$ achieved at c.m. energy $\sqrt{s} = 3.773 \text{ GeV}$. BESIII has collected large data samples in this energy region [33]. The cylindrical core of the BESIII detector covers 93% of the full solid angle and consists of a helium-based multilayer drift chamber (MDC), a time-of-flight system (TOF), and a CsI(Tl) electromagnetic calorimeter (EMC), which are all enclosed in a superconducting solenoidal magnet providing a 1.0 T magnetic field. The solenoid is supported by an octagonal flux-return yoke with resistive plate counter muon identification modules interleaved with steel. The charged-particle momentum resolution at 1 GeV/c is 0.5%, and the dE/dx resolution is 6% for electrons from Bhabha scattering. The EMC measures photon energies with a resolution of 2.5% (5%) at 1 GeV in the barrel (end cap) region. The time resolution in the plastic scintillator TOF barrel region is 68 ps, while that in the end cap region was 110 ps. The end cap TOF system was upgraded in 2015 using multi-

gap resistive plate chamber technology, providing a time resolution of 60 ps, which benefits 83% of the data used in this analysis [34].

The Monte Carlo (MC) simulation samples are generated using a GEANT4-based software package [35], incorporating a detailed geometric description of the BESIII detector and its response. These simulations are crucial for evaluating detection efficiencies, optimizing event selection criteria, and estimating background contributions. At each energy point, 100,000 signal events are generated for both processes $e^+e^- \rightarrow \gamma X(3872) \rightarrow \gamma K_S^0 K^\pm \pi^\mp$ and $e^+e^- \rightarrow \gamma X(3872) \rightarrow \gamma K^*(892)\bar{K}$. The $e^+e^- \rightarrow \gamma X(3872)$ is modeled as an E1 radiative transition, consistent with BESIII experimental data [6]. Initial state radiation (ISR) is simulated with KKMC [36], by incorporating the \sqrt{s} -dependent production cross section of $e^+e^- \rightarrow \gamma X(3872)$ into the program [13], where the energies of ISR photons range up to the values at the production threshold of the $\gamma X(3872)$ system.

The $X(3872) \rightarrow K_S^0 K^\pm \pi^\mp$ and $X(3872) \rightarrow K^*(892)\bar{K}$ decays are described with the phase-space model in EVTGEN [37]. Subsequent decays, $K^*(892)^0(\bar{K}^*(892)^0) \rightarrow K^+\pi^-(K^-\pi^+)$ and $K^*(892)^+(K^*(892)^-) \rightarrow K^0\pi^+(\bar{K}^0\pi^-)$, are modeled with the VSS model in EVTGEN which describes the decay of a vector particle into two scalars. The $K^*(892)^+K^- + \text{c.c.}$ and $K^*(892)^0\bar{K}^0 + \text{c.c.}$ processes are simulated together and are assumed to be produced at the same rate, which is consistent with isospin conservation. The decay $K_S^0 \rightarrow \pi^+\pi^-$ is also modeled using the phase-space approach. Final state radiation is simulated with PHOTOS [38].

To investigate potential background contributions, inclusive MC samples are utilized. These samples encompass open charm processes, ISR production of vector charmonium(-like) states, and continuum processes, all simulated with KKMC [36]. Particle decays are generated using EVTGEN [37], with branching fractions sourced from the Particle Data Group [7] when available, and otherwise modeled with LUNDCHARM [39] for charmonium states and PYTHIA [40] for other hadrons.

III. EVENT SELECTION AND BACKGROUND ANALYSIS

Charged tracks detected in the MDC are required to be within a polar angle (θ) range of $|\cos\theta| < 0.93$, where θ is defined with respect to the z -axis, which is the symmetry axis of the MDC. Particle identification (PID) for charged tracks combines measurements of the energy deposited in the MDC (dE/dx) and the flight time in the TOF to form likelihoods $\mathcal{L}(h)$ for each hadron hypothesis $h = p, K, \pi$. A track is classified as a kaon if $\mathcal{L}(K) > \mathcal{L}(p)$ and $\mathcal{L}(K) > \mathcal{L}(\pi)$. Identified kaons must satisfy vertex requirements: $V_r < 1.0$ cm and $|V_z| < 10.0$ cm, where V_r and V_z are the closest distances of charged tracks to the IP in the plane perpendicular to and along the beam direction, respectively. All remaining charged tracks are treated as pion candidates. Selected events must contain exactly one identified kaon and three pion candi-

dates, with a total charge of the four tracks summing to zero.

Photon candidates are identified from isolated showers in the EMC. Each shower must have a deposited energy exceeding 25 MeV in the barrel region ($|\cos\theta| < 0.80$) or 50 MeV in the end cap region ($0.86 < |\cos\theta| < 0.92$). To exclude showers produced by charged tracks, the angle between the EMC shower and the extrapolated position of the closest charged track at the EMC, measured from the interaction point (IP), must be greater than 10 degrees. To suppress electronic noise and showers unrelated to the collision event, the difference between the EMC shower time and the event start time must lie within [0, 700] ns. Events with at least one photon candidate meeting the above criteria are selected.

The K_S^0 candidates are reconstructed from pairs of oppositely charged pion tracks ($\pi^+\pi^-$) selected from the three pion candidates. All such pairs are subjected to a secondary vertex fit, ensuring the tracks originate from a common vertex. The invariant mass of these pairs must satisfy $|M_{\pi^+\pi^-} - m_{K_S^0}| < 22$ MeV/ c^2 , where $M_{\pi^+\pi^-}$ denotes the invariant mass of the $\pi^+\pi^-$ combination and $m_{K_S^0}$ is the K_S^0 nominal mass [7]. The decay length of the K_S^0 candidate, measured relative to the IP, must exceed twice the resolution of the vertex position. If more than one $\pi^+\pi^-$ combination in an event satisfies the above criteria, the combination with the least secondary vertex fit chi-square value is retained for further analysis. To estimate the background from non- K_S^0 processes, we use the events in the K_S^0 sideband regions defined by $0.432 < M_{\pi^+\pi^-} < 0.454$ GeV/ c^2 and $0.542 < M_{\pi^+\pi^-} < 0.564$ GeV/ c^2 . After reconstructing the K_S^0 , one pion candidate remains, which must satisfy the vertex constraints $V_r < 1.0$ cm and $|V_z| < 10.0$ cm.

Signal event candidates are identified as those containing four charged tracks, specifically one kaon, one additional pion, and the two pions originating from the K_S^0 , as well as at least one photon candidate. A vertex fit is further performed on the kaon, the additional pion, and the K_S^0 to confirm they originate from a common vertex at the IP. To enhance momentum resolution and suppress backgrounds, a four-momentum constraining kinematic fit (4C-fit) is applied to each signal event candidate, enforcing energy and momentum conservation with the initial e^+e^- collision system. Only events with a χ_{4C}^2 value less than 50 are retained, where χ_{4C}^2 represents the chi-square value from the 4C-fit for the signal hypothesis. In events with multiple possible combinations (e.g., multiple photons), the combination yielding the smallest χ_{4C}^2 is selected for further analysis.

To suppress backgrounds from processes without a photon, such as $e^+e^- \rightarrow K_S^0 K \pi$, a 4C-fit is performed to the background hypothesis with four tracks and no photon, and the resulting chi-square, $\chi_{4C,-\gamma}^2$, is required to be greater than χ_{4C}^2 . Similarly, to suppress backgrounds with an additional photon, we impose $\chi_{4C}^2 < \chi_{4C,+\gamma}^2$, where $\chi_{4C,+\gamma}^2$ denotes the chi-square from a fit for a hypothesis with an extra photon.

Background events containing a π^0 arise from processes such as $e^+e^- \rightarrow \gamma^{\text{ISR}} \pi^0 K_S^0 K^\pm \pi^\mp$ and $e^+e^- \rightarrow \gamma^{\text{ISR}} \rho^+ K^0 K^- + \text{c.c.}$, with $\rho^+ \rightarrow \pi^0 \pi^+$ and $K^0 \rightarrow K_S^0$. For the signal process $X(3872) \rightarrow K_S^0 K^\pm \pi^\mp$, a photon recoils

against the $K_S^0 K^\pm \pi^\mp$ system, and thus the invariant mass squared $M_{\text{recoil}}^2(K_S^0 K^\pm \pi^\mp)$ of the recoil system is expected to be zero. To eliminate the remaining π^0 backgrounds, we require that $M_{\text{recoil}}^2(K_S^0 K^\pm \pi^\mp) < 0.012 \text{ (GeV}/c^2)^2$.

The decay channels $X(3872) \rightarrow K_S^0 K^\pm \pi^\mp$ and $X(3872) \rightarrow K^*(892) \bar{K}$ share the same final state of $K_S^0 K^\pm \pi^\mp$, and thus the same event selection criteria described above applies to both channels. For the $X(3872) \rightarrow K^*(892) \bar{K}$ decay, additional requirements are imposed to select $K^*(892)$ candidates. Specifically, the invariant mass of the $K^\pm \pi^\mp$ pair must satisfy $0.748 < M_{K^\pm \pi^\mp} < 1.036 \text{ GeV}/c^2$ (three times the $K^*(892)^0$ width) to identify $K^*(892)^0$ or $\bar{K}^*(892)^0$ candidates, or the invariant mass of the $K_S^0 \pi^\pm$ pair must fall within $0.743 < M_{K_S^0 \pi^\pm} < 1.05 \text{ GeV}/c^2$ (three times the $K^*(892)^\pm$ width) to select $K^*(892)^\pm$ candidates. Figure 1 displays the invariant mass distribution of the $K_S^0 K^\pm \pi^\mp$ and $K^*(892) \bar{K}$ systems for all data sets combined after applying the event selection criteria.

IV. SIGNAL EXTRACTION AND CROSS SECTION MEASUREMENT

To extract the signal yield, an unbinned maximum likelihood fit is applied to the invariant mass distribution of $K_S^0 K^\pm \pi^\mp$ or $K^*(892) \bar{K}$. The signal probability density function (PDF) is modeled by convolving the $X(3872)$ signal shape, derived from the MC simulation, with a Gaussian function. This Gaussian function accounts for the mass resolution differences between the MC simulation and the data. Its mean and width parameters are fixed to values determined from a control sample of $\psi(2S) \rightarrow \gamma \chi_{c1}$, with $\chi_{c1} \rightarrow K_S^0 K^\pm \pi^\mp$, sharing the same final state as the signal process. The background is described using a second-order Chebychev polynomial function. Figure 1 displays the fitted curves overlaid on the data for the decay channels $X(3872) \rightarrow K_S^0 K^\pm \pi^\mp$ and $X(3872) \rightarrow K^*(892) \bar{K}$, with the fit results showing no significant signal for the $X(3872)$ in either channel.

The upper limit at the 90% confidence level (C.L.) for the signal yield of $X(3872)$ at each c.m. energy, N^{UL} , is calculated employing a Bayesian approach [41]. This method involves scanning the likelihood function over assumed signal event counts from zero to a sufficiently large upper bound, and defining the upper limit as the point where the integrated likelihood reaches 90% of the total probability. By excluding negative signal yields, this approach ensures a conservative estimation. These upper limits on the signal yields are subsequently converted into corresponding upper limits on the product of the cross section $\sigma[e^+e^- \rightarrow \gamma X(3872)]$ and branching fractions $\mathcal{B}[X(3872) \rightarrow K_S^0 K^\pm \pi^\mp]$ or $\mathcal{B}[X(3872) \rightarrow K^*(892) \bar{K}]$ using the following expressions:

$$\begin{aligned} \sigma^{\text{UL}}[e^+e^- \rightarrow X(3872)] \cdot \mathcal{B}[X(3872) \rightarrow K_S^0 K^\pm \pi^\mp / K^* \bar{K}] \\ = \frac{N^{\text{UL}}}{\mathcal{L}_{\text{int}}(1 + \delta)\varepsilon\mathcal{B}}. \end{aligned} \quad (1)$$

Here, ε is the selection efficiency; for decay channel $X(3872) \rightarrow K_S^0 K^\pm \pi^\mp$, \mathcal{B} is the branching fraction for

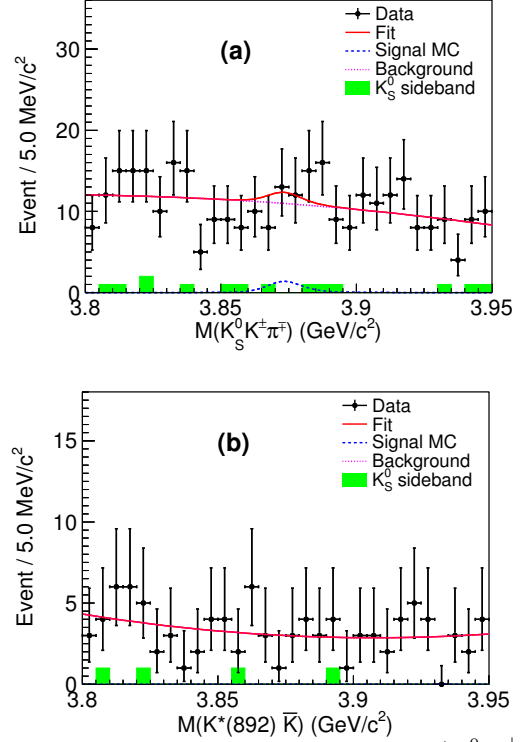


FIG. 1. Fits to the invariant mass distributions of $M(K_S^0 K^\pm \pi^\mp)$ and $M(K^* \bar{K})$ from data for the channels (a) $X(3872) \rightarrow K_S^0 K^\pm \pi^\mp$ and (b) $X(3872) \rightarrow K^*(892) \bar{K}$. The dots with error bars represent the full data set for all c.m. energies combined. The blue dashed curves are the signal PDFs, the red solid curves are the total fit results, the pink dashed curves represent the background components, and the green shaded histograms show the background estimated from the K_S^0 sideband region (in the lower plot, the fitted signal yield is negligible, rendering the signal PDFs essentially invisible and causing the background to nearly coincide with the total fit; consequently, the blue and pink curves are barely distinguishable).

$K_S^0 \rightarrow \pi^+ \pi^-$; for decay channel $X(3872) \rightarrow K^*(892) \bar{K}$, \mathcal{B} is a product of branching fractions involving the decays in the $K^*(892) \bar{K}$ channel: $K^*(892)^+(K^*(892)^-) \rightarrow K^0 \pi^+(\bar{K}^0 \pi^-)$, $K^*(892)^0(K^*(892)^0) \rightarrow K^+ \pi^-(K^- \pi^+)$, $K^0(\bar{K}^0) \rightarrow K_S^0$, and $K_S^0 \rightarrow \pi^+ \pi^-$; \mathcal{L}_{int} is the integrated luminosity; $(1 + \delta)$ accounts for the radiative corrections [13, 48].

Table I provides the upper limits on the product of the cross section and branching fractions for the decay channels $X(3872) \rightarrow K_S^0 K^\pm \pi^\mp$ and $X(3872) \rightarrow K^*(892) \bar{K}$, at each c.m. energy. Systematic uncertainties have been incorporated into the upper limit calculations.

V. RELATIVE BRANCHING RATIO MEASUREMENT

Since the decay channel $X(3872) \rightarrow \pi^+ \pi^- J/\psi$ has been well measured by the BESIII experiment [6], we also determine the relative branching ratios $\mathcal{R}_1 \equiv \frac{\mathcal{B}[X(3872) \rightarrow K_S^0 K^\pm \pi^\mp]}{\mathcal{B}[X(3872) \rightarrow \pi^+ \pi^- J/\psi]}$, and $\mathcal{R}_2 \equiv \frac{\mathcal{B}[X(3872) \rightarrow K^*(892) \bar{K}]}{\mathcal{B}[X(3872) \rightarrow \pi^+ \pi^- J/\psi]}$,

TABLE I. Upper limits at 90% C.L. for the measurement of the product of the cross section and branching ratio, $\sigma[e^+e^- \rightarrow \gamma X(3872)] \cdot \mathcal{B}[X(3872) \rightarrow K_S^0 K^\pm \pi^\mp]$ and $\sigma[e^+e^- \rightarrow \gamma X(3872)] \cdot \mathcal{B}[X(3872) \rightarrow K^*(892)\bar{K}]$, at different c.m. energies. The table includes the integrated luminosity \mathcal{L}_{int} , upper limit on the number of signal events N_1 and N_2 (where the subscript 1 denotes the $X(3872) \rightarrow K_S^0 K^\pm \pi^\mp$ process, and the subscript 2 represents the $X(3872) \rightarrow K^*(892)\bar{K}$ process), detection efficiencies ε_1 and ε_2 , radiative correction factor $(1 + \delta)$, upper limit on $\sigma_1 \cdot \mathcal{B}_1$ and $\sigma_2 \cdot \mathcal{B}_2$. Systematic uncertainties are incorporated into the upper limits.

$E_{\text{c.m.}}(\text{GeV})$	$\mathcal{L}_{\text{int}}(\text{pb}^{-1})$	N_1	N_2	$\varepsilon_1(\%)$	$\varepsilon_2(\%)$	$(1 + \delta)$	$\sigma_1 \cdot \mathcal{B}_1(\text{pb})$	$\sigma_2 \cdot \mathcal{B}_2(\text{pb})$
4.157	408.2	< 5.8	< 2.4	20.8	18.0	0.76	< 0.13	< 0.19
4.178	3194.5	< 10.7	< 4.6	21.8	20.8	0.76	< 0.03	< 0.04
4.189	526.7	< 7.5	< 4.0	21.9	20.8	0.77	< 0.13	< 0.21
4.199	526.0	< 5.5	< 3.9	21.5	20.8	0.78	< 0.09	< 0.20
4.209	517.1	< 5.2	< 3.8	21.0	19.9	0.80	< 0.09	< 0.20
4.219	514.6	< 6.4	< 5.4	20.7	19.5	0.82	< 0.11	< 0.29
4.226	1056.4	< 5.3	< 6.0	21.1	20.0	0.84	< 0.04	< 0.15
4.236	530.3	< 5.1	< 5.3	20.1	19.2	0.86	< 0.08	< 0.26
4.244	538.1	< 3.1	< 3.8	19.6	18.6	0.89	< 0.05	< 0.19
4.258	828.4	< 5.2	< 5.0	18.7	17.8	0.93	< 0.06	< 0.16
4.267	531.1	< 7.4	< 2.7	18.1	17.3	0.96	< 0.12	< 0.14
4.278	175.7	< 4.0	< 3.9	16.9	16.1	0.99	< 0.20	< 0.61
4.288	502.4	< 5.1	< 3.1	15.5	13.7	1.02	< 0.10	< 0.20
4.312	501.1	< 2.7	< 2.7	14.5	12.5	1.09	< 0.05	< 0.18
4.337	504.9	< 7.1	< 5.3	13.4	11.9	1.16	< 0.13	< 0.33

which are calculated using the equations:

$$\mathcal{R}_1 = \frac{N_{K_S^0 K^\pm \pi^\mp}}{N_{\pi^+ \pi^- J/\psi}} \cdot \frac{\varepsilon_{\pi^+ \pi^- J/\psi}^{\text{ave}}}{\varepsilon_{K_S^0 K^\pm \pi^\mp}^{\text{ave}}} \cdot \frac{\mathcal{B}(J/\psi \rightarrow l^+ l^-)}{\mathcal{B}} \quad (2)$$

and

$$\mathcal{R}_2 = \frac{N_{K^*(892)\bar{K}}}{N_{\pi^+ \pi^- J/\psi}} \cdot \frac{\varepsilon_{\pi^+ \pi^- J/\psi}^{\text{ave}}}{\varepsilon_{K^*(892)\bar{K}}^{\text{ave}}} \cdot \frac{\mathcal{B}(J/\psi \rightarrow l^+ l^-)}{\mathcal{B}} \quad (3)$$

Here, $N_{K_S^0 K^\pm \pi^\mp}$ and $N_{K^*(892)\bar{K}}$ represent the total number of signal events for the decay channels $X(3872) \rightarrow K_S^0 K^\pm \pi^\mp$ and $X(3872) \rightarrow K^*(892)\bar{K}$, derived by fitting the combined data samples across all energies; $N_{\pi^+ \pi^- J/\psi} = 86.3^{+10.5}_{-9.8}$ is the number of signal events in the normalization channel $X(3872) \rightarrow \pi^+ \pi^- J/\psi$, as reported in Ref. [6]; $\varepsilon_{K_S^0 K^\pm \pi^\mp}^{\text{ave}}$ and $\varepsilon_{K^*(892)\bar{K}}^{\text{ave}}$ denotes the averaged detection efficiency for the decay channels $X(3872) \rightarrow K_S^0 K^\pm \pi^\mp$ and $X(3872) \rightarrow K^*(892)\bar{K}$; $\varepsilon_{\pi^+ \pi^- J/\psi}^{\text{ave}}$ is the averaged detection efficiency for the normalization channel $X(3872) \rightarrow \pi^+ \pi^- J/\psi$, calculated using efficiencies from Ref. [6]; $\mathcal{B}(J/\psi \rightarrow l^+ l^-)$ is the branching fraction of $J/\psi \rightarrow l^+ l^-$ ($l = e$ or μ); \mathcal{B} represents the product of branching fractions for the specific decay channels, consistent with the cross section measurement. The averaged efficiencies ($\varepsilon_{K_S^0 K^\pm \pi^\mp}^{\text{ave}}$, $\varepsilon_{K^*(892)\bar{K}}^{\text{ave}}$ and $\varepsilon_{\pi^+ \pi^- J/\psi}^{\text{ave}}$) are calculated by weighting the efficiencies at each energy by the integrated luminosity and the production cross section of $e^+e^- \rightarrow \gamma X(3872)$.

In the absence of a significant signal in the decay channels $X(3872) \rightarrow K_S^0 K^\pm \pi^\mp$ and $X(3872) \rightarrow K^*(892)\bar{K}$, upper limits on the signal yields for the combined data samples are established at the 90% C.L.: $N < 23.0$ for $X(3872) \rightarrow$

$K_S^0 K^\pm \pi^\mp$ and $N < 10.7$ for $X(3872) \rightarrow K^*(892)\bar{K}$. Applying Eq. (3), the corresponding upper limits on the relative branching ratios are $\mathcal{R}_1 < 0.07$ and $\mathcal{R}_2 < 0.10$, respectively, with systematic uncertainties considered.

VI. SYSTEMATIC UNCERTAINTY

The systematic uncertainties in the measurement of the cross section arise from multiple sources, including the integrated luminosity, photon detection efficiency, K_S^0 reconstruction, charged track reconstruction, PID, kinematic fit, MC decay model, radiative correction, background veto, branching fractions, and signal extraction. The systematic uncertainties mentioned above can be broadly classified into two categories: additive and multiplicative. The signal extraction is classified as an additive systematic uncertainty, while the remaining sources are categorized as multiplicative systematic uncertainties.

The integrated luminosity is determined using large-angle Bhabha scattering events, with a systematic uncertainty of 0.7% [42].

The photon detection efficiency contributes a systematic uncertainty of 1.0%, as established in Ref. [43].

The systematic uncertainty associated with the K_S^0 reconstruction efficiency is assessed using control samples $J/\psi \rightarrow K^{*\pm} K^\mp$ and $J/\psi \rightarrow K_S^0 K^\pm \pi^\mp$ [44]. This uncertainty, which includes the pion tracking efficiency and the K_S^0 mass window selection, is quantified as 1.2% based on differences between data and MC simulation.

The tracking efficiency for charged particles originating

from the IP introduces a systematic uncertainty. For the single kaon and pion tracks, each contributes a 1.0% uncertainty, yielding a total tracking uncertainty of 2.0% [45].

The PID is applied solely to the kaon track, with a systematic uncertainty of 1.0% in the PID efficiency, as reported in Ref. [46].

To address discrepancies in track helix parameters between data and MC simulations, a correction method is implemented during the kinematic fit, following Ref. [47]. The systematic uncertainty from the kinematic fit is conservatively estimated as the difference in detection efficiencies between corrected and uncorrected MC samples.

For the $X(3872) \rightarrow K_S^0 K^\pm \pi^\mp$ decay channel, the nominal MC model employs a phase space distribution. An alternative model, inspired by the decay of the χ_{c1} state [7] with identical $J^{PC} = 1^{++}$ quantum numbers, assumes the $X(3872)$ decays via intermediate $K^*(892)\bar{K}$ resonance states, subsequently producing the $K_S^0 K^\pm \pi^\mp$ final state. The systematic uncertainty due to the MC decay model is determined by comparing detection efficiencies between the nominal phase space model and this alternative resonance-based model.

Similarly, for the $X(3872) \rightarrow K^*(892)\bar{K}$ channel, which also results in the $K_S^0 K^\pm \pi^\mp$ final state, the nominal model assumes an equal ratio of $K^*(892)^+ K^- + c.c.$ and $K^*(892)^0 \bar{K}^0 + c.c.$, as predicted by isospin symmetry. The alternative resonance-based approach adopts the Body3 model [37], incorporating the possible decay dynamics of the χ_{c1} state and accounting for intermediate $K^*(892)$ resonances. This model generates three-body $K_S^0 K^\pm \pi^\mp$ events using the Dalitz plot and angular distributions from χ_{c1} data. The systematic uncertainty is evaluated as the difference in detection efficiencies between the nominal and alternative models.

The radiative correction factor is computed using the method in Ref. [48], derived from the cross-section line shape of $e^+e^- \rightarrow \gamma X(3872)$ [13]. The line shape is modeled with a Breit-Wigner function for the $Y(4200)$ resonance, characterized by a mass of $M = 4200.6_{-13.3}^{+7.9} \pm 3.0$ MeV/ c^2 and a width of $\Gamma = 115_{-26}^{+38} \pm 12$ MeV. To estimate the uncertainty in the radiative correction due to these resonance parameters, a two-dimensional Gaussian sampling method is employed. Specifically, 300 sets of mass and width parameters for the $Y(4200)$ are generated, and for each set, the product $(1 + \delta)\epsilon$ is recalculated using the weight method from Ref. [48]. The relative standard deviation of the resulting $(1 + \delta)\epsilon$ distribution, expressed as a percentage, is taken as the systematic uncertainty.

The systematic uncertainty from the π^0 veto criterion, defined as $M_{\text{recoil}}^2(K_S^0 K^\pm \pi^\mp) < 0.012$ (GeV/ c^2)², is related to the photon energy (the efficiency loss induced by π^0 veto criterion exhibits a direct positive correlation with photon energy). To estimate the systematic uncertainty associated with this criterion, control samples are selected from the $\psi(2S) \rightarrow \gamma \chi_{c1}$ and $e^+e^- \rightarrow \gamma^{\text{ISR}} J/\psi$ (at 3.773 GeV, 4.178 GeV and 4.226 GeV) processes. These processes provide photons with varying energies. Efficiency differences between MC simulations and data sets are analyzed, and we extrapolate the sys-

tematic uncertainty to our studied signal process.

The background veto criterion $\chi_{4C}^2 < \chi_{4C,\pm\gamma}^2$ introduces a systematic uncertainty, assessed using the control sample $\psi(2S) \rightarrow \gamma \chi_{c1} \rightarrow \gamma K_S^0 K^\pm \pi^\mp$. The efficiency difference between signal MC simulations and data is 0.1%, and is deemed negligible. Given the high precision of the branching fractions for $K_S^0 \rightarrow \pi^+ \pi^-$ and relevant $K^*(892)$ decays [7], their uncertainties are negligible and omitted from the total systematic uncertainty.

Assuming the above systematic uncertainties are independent, the total multiplicative systematic uncertainty σ_{multi} is calculated by summing the individual contributions in quadrature. The results are summarized in Table II.

The systematic uncertainty in signal extraction stems from the signal shape, background shape, and fit range. The signal shape uncertainty is addressed by varying the width parameter of the convolved Gaussian function within one standard deviation. The uncertainty due to the background shape is evaluated by switching from a second-order to a first-order polynomial function. The uncertainty due to fit range is assessed by adjusting the range by ± 10 MeV. The most conservative signal yield, accounting for these combined effects, is adopted as the final result.

To take into account the multiplicative systematic uncertainty, the likelihood curve is further convolved by a Gaussian with a width parameter equal to the total multiplicative systematic uncertainty $\int_0^{+\infty} \mathcal{L}(N'_{\text{sig}}) e^{-\frac{(N_{\text{sig}} - N'_{\text{sig}})^2}{2(\sigma_{\text{multi}} N_{\text{sig}})^2}} dN'_{\text{sig}}$, where $N_{\text{sig}}^{(\prime)}$ is the signal yield and $\mathcal{L}(N'_{\text{sig}})$ is the likelihood function. The final result is based on the most conservative upper limit estimate, with all systematic uncertainties taken into account.

The systematic uncertainties for \mathcal{R}_1 and \mathcal{R}_2 align with those of the cross-section measurement. However, since it is a ratio measurement, several uncertainties cancel, including those from integrated luminosity, photon detection, tracking efficiency, kinematic fit, and radiative correction. The remaining uncertainties for the search channels $X(3872) \rightarrow K_S^0 K^\pm \pi^\mp$ and $X(3872) \rightarrow K^*(892)\bar{K}$ arise from the PID, MC decay model, K_S^0 reconstruction, and π^0 veto, totaling 5.4% and 7.0%, respectively. For the normalization channel $X(3872) \rightarrow \pi^+ \pi^- J/\psi$, remaining uncertainties stem from the statistical uncertainty of $N_{\pi^+ \pi^- J/\psi}$, the branching fraction $\mathcal{B}(J/\psi \rightarrow l^+ l^-)$, and the J/ψ mass window, totaling 12.4% [49, 50]. The total systematic uncertainties for the ratio measurements are 13.5% for \mathcal{R}_1 and 14.2% for \mathcal{R}_2 .

VII. SUMMARY

In this paper, we investigate the decays $X(3872) \rightarrow K_S^0 K^\pm \pi^\mp$ and $X(3872) \rightarrow K^*(892)\bar{K}$, where the $X(3872)$ is produced through the process $e^+e^- \rightarrow \gamma X(3872)$, utilizing data collected by the BESIII detector at c.m. energies ranging from 4.16 to 4.34 GeV. No significant signals are observed for either decay mode. As a result, we es-

TABLE II. Systematic uncertainties (in percent) for the measurement of $\sigma(e^+e^- \rightarrow \gamma X(3872)) \cdot \mathcal{B}(X(3872) \rightarrow K_S^0 K^\pm \pi^\mp)$ and $\sigma(e^+e^- \rightarrow \gamma X(3872)) \cdot \mathcal{B}(X(3872) \rightarrow K^*(892)\bar{K})$ (values in parentheses). The total systematic uncertainty is the quadrature sum of individual contributions.

$E_{\text{c.m.}}$ (GeV)	Luminosity	Photon Tracking	PID	Kinematic fit	$(1 + \delta)$	MC model	K_S^0 rec.	π^0 veto	Total (%)
4.157	0.7	1.0	2.0	1.0	1.7 (1.2)	0.1	0.4 (5.3)	1.2	4.3 (3.2) 5.4 (6.9)
4.178	0.7	1.0	2.0	1.0	0.7 (1.0)	0.8	2.4 (4.6)	1.2	4.3 (3.2) 5.2 (6.3)
4.189	0.7	1.0	2.0	1.0	0.9 (0.9)	1.1	0.4 (5.0)	1.2	4.3 (3.2) 4.8 (6.3)
4.199	0.7	1.0	2.0	1.0	1.2 (1.1)	0.9	2.5 (5.8)	1.2	4.3 (3.2) 5.6 (7.0)
4.209	0.7	1.0	2.0	1.0	1.2 (1.2)	0.9	1.5 (4.9)	1.2	4.3 (3.2) 5.3 (6.2)
4.219	0.7	1.0	2.0	1.0	1.0 (1.2)	1.0	0.3 (5.0)	1.2	4.3 (3.2) 4.9 (6.3)
4.226	0.7	1.0	2.0	1.0	1.1 (1.2)	0.8	1.1 (5.7)	1.2	4.3 (3.2) 5.0 (6.6)
4.236	0.7	1.0	2.0	1.0	1.0 (1.1)	1.0	1.2 (4.7)	1.2	4.3 (3.2) 5.1 (6.0)
4.244	0.7	1.0	2.0	1.0	1.2 (1.1)	0.9	1.8 (4.2)	1.2	4.3 (3.2) 5.4 (5.7)
4.258	0.7	1.0	2.0	1.0	1.2 (1.1)	0.9	2.0 (6.0)	1.2	4.3 (3.2) 5.5 (6.9)
4.267	0.7	1.0	2.0	1.0	1.3 (1.1)	1.1	0.9 (4.8)	1.2	4.3 (3.2) 5.0 (6.0)
4.278	0.7	1.0	2.0	1.0	1.0 (1.3)	1.0	2.9 (2.8)	1.2	4.3 (3.2) 5.7 (5.0)
4.288	0.7	1.0	2.0	1.0	1.5 (1.7)	0.9	0.4 (5.0)	1.2	4.3 (3.2) 5.4 (6.6)
4.312	0.7	1.0	2.0	1.0	1.7 (1.2)	0.6	0.8 (3.6)	1.2	4.3 (3.2) 5.5 (5.3)
4.337	0.7	1.0	2.0	1.0	1.2 (1.4)	0.6	1.2 (4.0)	1.2	4.3 (3.2) 5.4 (5.6)

timate upper limits at the 90% C.L. on the product of the production cross section and branching fractions, denoted as $\sigma[e^+e^- \rightarrow \gamma X(3872)] \cdot \mathcal{B}[X(3872) \rightarrow K_S^0 K^\pm \pi^\mp]$ and $\sigma[e^+e^- \rightarrow \gamma X(3872)] \cdot \mathcal{B}[X(3872) \rightarrow K^*(892)\bar{K}]$, across the specified energy range.

Furthermore, we evaluate the relative branching fractions of these decay channels compared to the well-established decay $X(3872) \rightarrow \pi^+\pi^-J/\psi$. These ratios are determined as $\mathcal{R}_1 = \frac{\mathcal{B}(X(3872) \rightarrow K_S^0 K^\pm \pi^\mp)}{\mathcal{B}(X(3872) \rightarrow \pi^+\pi^-J/\psi)} < 0.07$ and $\mathcal{R}_2 = \frac{\mathcal{B}(X(3872) \rightarrow K^*(892)\bar{K})}{\mathcal{B}(X(3872) \rightarrow \pi^+\pi^-J/\psi)} < 0.10$ at the 90% C.L. For the decay $X(3872) \rightarrow K^*(892)\bar{K}$, using the branching fraction $\mathcal{B}(X(3872) \rightarrow \pi^+\pi^-J/\psi) = (4.3 \pm 1.4)\%$ from the PDG [7], we derive an upper limit on the branching fraction of $\mathcal{B}[X(3872) \rightarrow K^*(892)\bar{K}] < 0.60 \times 10^{-2}$. Our upper limit falls within the lower region of the theoretical prediction ranges, providing significant constraints on the intermediate charmed meson loops model parameter α [30]. This is not only of significant importance to the theoretical calculations of $X(3872) \rightarrow VP$ and $X(3872) \rightarrow VV$, but also provides insights into the nature of the $X(3872)$.

Acknowledgement

The BESIII Collaboration thanks the staff of BEPCII (<https://cstr.cn/31109.02.BEPC>) and the IHEP computing center for their strong support. This work is supported in

part by National Key R&D Program of China under Contracts Nos. 2023YFA1606000, 2023YFA1606704; National Natural Science Foundation of China (NSFC) under Contracts Nos. 11635010, 11935015, 11935016, 11935018, 12025502, 12035009, 12035013, 12061131003, 12192260, 12192261, 12192262, 12192263, 12192264, 12192265, 12221005, 12225509, 12235017, 12361141819; the Chinese Academy of Sciences (CAS) Large-Scale Scientific Facility Program; the Strategic Priority Research Program of Chinese Academy of Sciences under Contract No. XDA0480600; CAS under Contract No. YSBR-101; 100 Talents Program of CAS; Project ZR2022JQ02 supported by Shandong Provincial Natural Science Foundation; the Institute of Nuclear and Particle Physics (INPAC) and Shanghai Key Laboratory for Particle Physics and Cosmology; ERC under Contract No. 758462; German Research Foundation DFG under Contract No. FOR5327; Istituto Nazionale di Fisica Nucleare, Italy; Knut and Alice Wallenberg Foundation under Contracts Nos. 2021.0174, 2021.0299; Ministry of Development of Turkey under Contract No. DPT2006K-120470; National Research Foundation of Korea under Contract No. NRF-2022R1A2C1092335; National Science and Technology fund of Mongolia; Polish National Science Centre under Contract No. 2024/53/B/ST2/00975; STFC (United Kingdom); Swedish Research Council under Contract No. 2019.04595; U. S. Department of Energy under Contract No. DE-FG02-05ER41374

[1] S. K. Choi *et al.* [Belle Collaboration], *Phys. Rev. Lett.* **91**, 262001 (2003).
[2] D. Acosta *et al.* [CDF Collaboration], *Phys. Rev. Lett.* **93**, 072001 (2004).

[3] V. M. Abazov *et al.* [D0 Collaboration], *Phys. Rev. Lett.* **93**, 162002 (2004).
[4] B. Aubert *et al.* [BaBar Collaboration], *Phys. Rev. D* **71**, 071103 (2005).

- [5] R. Aaij *et al.* [LHCb Collaboration], *Phys. Rev. Lett.* **110**, 222001 (2013).
- [6] M. Ablikim *et al.* [BESIII Collaboration], *Phys. Rev. Lett.* **112**, 092001 (2014).
- [7] S. Navas *et al.* [Particle Data Group], *Phys. Rev. D* **110**, 030001 (2024).
- [8] R. Aaij *et al.* [LHCb Collaboration], *Phys. Rev. D* **92**, 011102 (2015).
- [9] T. Aushev *et al.* [Belle Collaboration], *Phys. Rev. D* **81**, 031103 (2010).
- [10] B. Aubert *et al.* [BaBar Collaboration], *Phys. Rev. D* **77**, 011102 (2008).
- [11] H. Hirata *et al.* [Belle Collaboration], *Phys. Rev. D* **107**, 112011 (2023).
- [12] M. Ablikim *et al.* [BESIII Collaboration], *Phys. Rev. Lett.* **124**, 242001 (2020).
- [13] M. Ablikim *et al.* [BESIII Collaboration], *Phys. Rev. Lett.* **122**, 232002 (2019).
- [14] T. Barnes and S. Godfrey, *Phys. Rev. D* **69**, 054008 (2004).
- [15] E. J. Eichten, K. Lane and C. Quigg, *Phys. Rev. D* **69**, 094019 (2004).
- [16] T. Barnes, S. Godfrey and E. S. Swanson, *Phys. Rev. D* **72**, 054026 (2005).
- [17] F. E. Close and P. R. Page, *Phys. Lett. B* **578**, 119-123 (2004).
- [18] S. Fleming, M. Kusunoki, T. Mehen and U. van Kolck, *Phys. Rev. D* **76**, 034006 (2007).
- [19] P. Wang and X. G. Wang, *Phys. Rev. Lett.* **111**, 042002 (2013).
- [20] L. Maiani, F. Piccinini, A. D. Polosa and V. Riquer, *Phys. Rev. D* **71**, 014028 (2005).
- [21] R. D. Matheus, S. Narison, M. Nielsen and J. M. Richard, *Phys. Rev. D* **75**, 014005 (2007).
- [22] Y. S. Kalashnikova, *Phys. Rev. D* **72**, 034010 (2005).
- [23] M. Takizawa and S. Takeuchi, *PTEP* **2013**, 093D01 (2013).
- [24] S. Coito, G. Rupp and E. van Beveren, *Eur. Phys. J. C* **71**, 1762 (2011).
- [25] J. P. Lees *et al.* [BaBar Collaboration], *Phys. Rev. D* **95**, 072007 (2017).
- [26] R. Aaij *et al.* [LHCb Collaboration], *Phys. Rev. D* **108**, 032010 (2023).
- [27] M. Ablikim *et al.* [BES Collaboration], *Phys. Rev. D* **74**, 072001 (2006).
- [28] M. Ablikim *et al.* [BESIII Collaboration], *Phys. Rev. D* **110**, 012007 (2024).
- [29] M. Ablikim *et al.* [BESIII Collaboration], *Phys. Rev. D* **96**, 111102 (2017).
- [30] Yan Wang, Qi Wu, Gang Li, Wen-Hua Qin, Xiao-Hai Liu, Chun-Sheng An, and Ju-Jun Xie, *Phys. Rev. D* **106**, 074015 (2022).
- [31] M. Ablikim *et al.* [BESIII Collaboration], *Nucl. Instrum. Meth. A* **614**, 345-399 (2010).
- [32] C. H. Yu *et al.*, *Proceedings of IPAC2016, Busan, Korea, 2016*.
- [33] M. Ablikim *et al.* [BESIII Collaboration], *Chin. Phys. C* **44**, 040001 (2020).
- [34] X. Li *et al.*, *Radiat. Detect. Technol. Methods* **1**, 13 (2017); Y. X. Guo *et al.*, *Radiat. Detect. Technol. Methods* **1**, 15 (2017); P. Cao *et al.*, *Nucl. Instrum. Meth. A* **953**, 163053 (2020).
- [35] S. Agostinelli *et al.* [GEANT4 Collaboration], *Nucl. Instrum. Meth. A* **506**, 250 (2003).
- [36] S. Jadach, B. F. L. Ward and Z. Was, *Phys. Rev. D* **63**, 113009 (2001); *Comput. Phys. Commun.* **130**, 260 (2000).
- [37] D. J. Lange, *Nucl. Instrum. Meth. A* **462**, 152 (2001); R. G. Ping, *Chin. Phys. C* **32**, 599 (2008).
- [38] E. Barberio, B. van Eijk and Z. Was, *Comput. Phys. Commun.* **66**, 115 (1991).
- [39] J. C. Chen, G. S. Huang, X. R. Qi, D. H. Zhang and Y. S. Zhu, *Phys. Rev. D* **62**, 034003 (2000); R. L. Yang, R. G. Ping and H. Chen, *Chin. Phys. Lett.* **31**, 061301 (2014).
- [40] T.Sjöstrand, S.Ask, J.R.Christiansen, R.Corke, N.Desai, P. Ilten, S.Mrenna, S.Prestel, C.O.Rasmussen, and P.Z.Skands, *Comput. Phys. Commun.* **191**, 159 (2015).
- [41] C. Rover, C. Messenger and R. Prix, doi:10.5170/CERN-2011-006.158.
- [42] M. Ablikim *et al.* [BESIII Collaboration], *Chin. Phys. C* **46**, 113002 (2022).
- [43] V. Prasad, C. Liu, X. Ji, W. Li, H. Liu and X. Lou, *Springer Proc. Phys.* **174**, 577-582 (2016).
- [44] M. Ablikim *et al.* [BESIII Collaboration], *Phys. Rev. D* **96**, 012001 (2017).
- [45] M. Ablikim *et al.* [BESIII Collaboration], *Phys. Rev. D* **83**, 112005 (2011).
- [46] M. Ablikim *et al.* [BESIII Collaboration], *Phys. Rev. D* **99**, 112010 (2019).
- [47] M. Ablikim *et al.* [BESIII Collaboration], *Phys. Rev. D* **87**, 012002 (2013).
- [48] W. Sun, T. Liu, M. Jing, L. Wang, B. Zhong and W. Song, *Front. Phys. (Beijing)* **16**, 64501 (2021).
- [49] M. Ablikim *et al.* [BESIII Collaboration], *Phys. Rev. D* **109**, L071101 (2024).
- [50] M. Ablikim *et al.* [BESIII Collaboration], *Phys. Rev. D* **109**, L011102 (2024).